Proceedings of CHT-17
ICHMT International Symposium on Advances in Computational Heat Transfer

May 28-June 1, 2017, Napoli, Italy

CHT-17-039

NUMERICAL SIMULATION OF FLOW TRANSITION IN A RECTANGULAR MICROCHANNEL

Cheng Jian[*], Li Haiwang [*,§], Zhu Zhibing[*] and Tao Zhi[*]
[*]National Key Laboratory of Science and Technology on Aero-Engine Aero-Thermodynamics,
School of Energy and Power Engineering,
Beihang University, Beijing 100191, China
[§]Correspondence author. Fax: +86 010 8231 4379 Email: 09620@buaa.edu.cn

ABSTRACT The behavior of flow transition in a rectangular microchannel was numerically investigated. In the simulation, three flow models were adopted, namely, a γ-$Re_{\theta t}$ transition model, a laminar model and a shear stress transport (SST) model. The simulation was conducted using ANSYS CFX, and the results were compared with experimental data, then the effect of length-to-diameter ratio (L/D) on the critical Reynolds number was studied. Results indicate that the laminar model and the γ-$Re_{\theta t}$ transition model produce similar pressure drops when the mass flow rate is smaller. When the mass flow rate increases, values predicted by the γ-$Re_{\theta t}$ transition model matches best with the experimental data. The laminar model and the SST model are incapable of predicting transition, while the γ-$Re_{\theta t}$ transition model forecasts the critical Reynolds number well and the predicted values match well with the experimental data. In the present study, the transition is accurately simulated and the flow mechanism is revealed. The results also show that local turbulent regions appear at the rear of the microchannel before the Reynolds number reaches the critical value and the turbulent regions expand with the increase of the Reynolds number. For microchannels with $L/D \geq 100$, the transition from laminar to turbulent regime occurs for a Reynolds number in the range 2000-2500, and the length-to-diameter ratio has no significant effect on the critical Reynolds number.

INTRODUCTION

Micro-Electro-Mechanical Systems (MEMS), which was proposed in the 1980s, are widely used in the fields of aeronautics, astronautics, bioengineering, and so forth. By now, the research about the basic theory and application has been in vogue all around the world. As an important branch of MEMS, the flow mechanism of fluid in microchannels attracts more and more attention because it determines the performance of MEMS. It has been observed that the flow behavior in microchannels is quite distinct from the predictions using conventional fluid mechanics theory, which consequently generates a growing demand for research.

Mala and Li [1999] conducted experiments to investigate the behavior of water flow in microtubes of stainless steel and fused silica with diameters ranging from 50 to 254 μm. The results indicated the friction factor at higher Reynolds number was bigger than that predicted by the conventional theory. The flow characteristics also exhibited material dependence. Moreover, the authors attributed the earlier transition to the effects of surface roughness.

Qu et al. [2000] reported their research work on the water flow behavior in trapezoidal microchannels. The experimental results showed a significant deviation from the predictions of conventional theory, including a higher pressure gradient and flow friction. The authors ascribed these phenomena to the effect of surface roughness. On this basis, a roughness-viscosity model was proposed which agreed well with the experimental data.

Toh et al. [2002] developed a numerical procedure based on the finite volume method (FVM) to study the flow behavior of water flows in the laminar regime in heated microchannels. The method was validated by comparing the numerical results with the experimental data of Tuckerman [1984].

Hu et al. [2003] developed a finite-volume-based numerical model to investigate the velocity distribution and the pressure drop in microchannels. The simulation results revealed that the height, size and spacing of the roughness elements all made a difference.

Rawool et al. [2006] numerically investigated the relationship between the friction factor and the roughness height, geometry and Reynolds number. It was observed that the friction factor of the rectangular and triangular obstructions is higher than the trapezoidal ones. The friction factor decreases with the increase of Reynolds number in a nonlinear trend and increase nonlinearly with the increase of the roughness height.

Mokrani et al. [2009] reported the conclusion from their experiments that for microchannels of channel heights between 50 and 500 μm, the conventional laws and correlations describing the flow in large-scale channels remained applicable. Moreover, no earlier transition was observed in the tests.

Zhang et al. [2014] measured the pressure drop in six multiport microchannel flat tubes with different geometry parameters and calculated the friction factor. In the experiments, an earlier transition was observed and the aspect ratio seems to correlate with that. Additionally, the entrance effect seemed to have a significant impact on the friction factor especially at higher Reynolds numbers.

Sahar et al. [2016] performed a numerical study with FLUENT to investigate the flow behavior of water and R134a in a single rectangular microchannel with different geometric models. The 2D model predicted a lower value for the friction factor while the 3D thin-wall model exhibited a transition change at $Re \approx 1600$, corresponding with the experimental data.

Over these years, the research on fluid flow in microchannels mainly focused either on the characteristics of the flows (such as the pressure drop through the microchannels, friction factor and the critical Reynolds number, etc.), or on the factors which have an impact on the behavior of the flows (such as compressibility, roughness, velocity slip and temperature jump, etc.). But

unfortunately, most of the investigations only described the overall and average behavior of microfluidics because the test technique is not enough to capture the details of flows in microfluidics. Moreover, the study on the flow mechanism in a single microchannel is not sufficient. In the case of numerical study, most investigators would use a laminar model for laminar flows or turbulence models without considering the transition in the channels. The present study attempts to introduce the transition model into the numerical simulation and to verify the validity of the model by comparing the predicted values with the experimental data. The entrance effect has an obvious influence on the flow characteristics in short microchannels as observed in short macrochannels, however, it is unclear to what extent the entrance region affects the flow behavior in microchannels with different lengths, so the effect of length-to-diameter ratio on the critical Reynolds number is also investigated.

NUMERICAL SIMULATION

Continuum Assumption By averaging the microscopic quantities on a small sampling volume, the continuum assumption erases the molecular discontinuities, which makes it very convenient for application [e.g., Kandlikar et al. 2005]. Many codes such as ANSYS CFX are programmed based on the continuum assumption.

Generally, the continuum assumption is applicable in the simulation of macroscopic fluid flow. However, the dimensions of the microchannels are very small, and sometimes it can even be on the same order of magnitude as the mean free path of fluid molecules. As a result, the validity of the continuum assumption is supposed to be considered prior to the numerical simulation of fluid flow in microchannels.

Typically, the flow is regarded as a continuum flow for $Kn<0.001$ [e.g., Tsien 1946] and that it can be accurately modeled by the Navier-Stokes equations with classical no-slip boundary conditions. In the present study, the maximum of Kn was 1.75×10^{-4}, thus the continuum assumption was valid.

Selection of Flow Models According to the experimental results, the critical Reynolds number is about 2100. To simulate transition, in addition to direct numerical simulation (DNS) and large eddy simulation (LES), transition models have been developing rapidly during the past years. Generally, four models are adopted in engineering application, namely, low Reynolds number models, models based on turbulence intermittency, laminar kinetic energy transition models and instability wave models.

In this paper, the γ-$Re_{\theta t}$ transition model based on intermittency was used to carry out the simulations. Furthermore, the laminar model and the SST model were also used for comparison.

Physical Model and Computational Domain The experiments involved in this simulation were carried out in a self-designed test rig as illustrated in Zhu et al. [2016] with a detailed depiction of the experiment setup and methods. There were 22 microchannels in the test piece and all channels were assumed to be the same. The length of every microchannel was 90 mm and the size of the cross section was 0.4 mm ×0.4 mm.

It would be extremely intensive if the computational model contained the whole test piece with 22

microchannels, hence a simplified computational domain was considered in this simulation, namely, only one microchannel was modeled. Additionally, the construction of a single microchannel clearly exhibited geometrical symmetry, so in consideration of all the simplifications above, only a quarter of a microchannel was chosen as the computational domain. Thus the computational domain was a cuboid domain with 0.2 mm width (*W*) and 0.2 mm height (*H*) and 90 mm length (*L*) as presented in Figure 1.

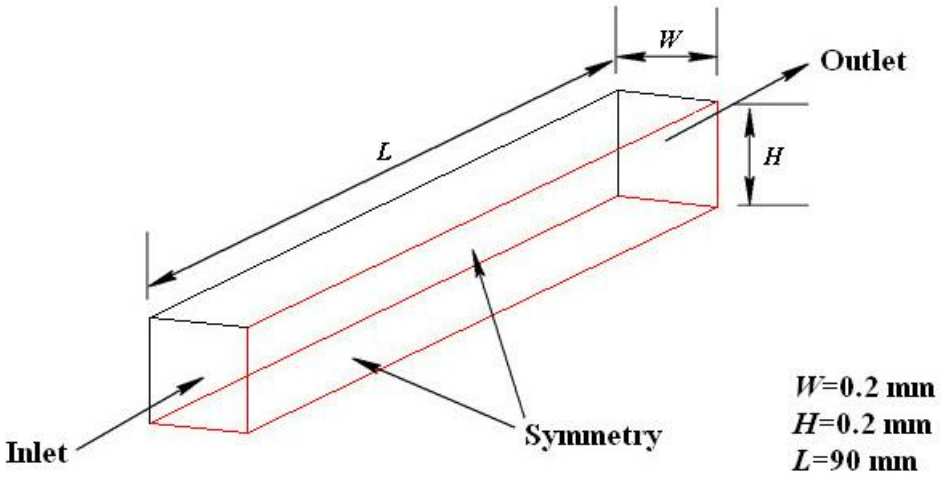

Figure 1. Computational domain used for the simulation

Grid Independence Analysis The gridding was carried out in ICEM. The geometric construction of the selected computational domain was straightforward, so structured hexahedral elements were adopted for high-quality grids. In order to achieve a balance between the solution accuracy and the computation time, grid independence was verified respectively for the three flow models. Taking the γ-$Re_{\theta t}$ transition model as an example, the case at Re=2000 is shown in Table 1, where N is the number of cells. Variables with subscript i and i-1 mean the values of parameters for the current grid and the last grid, respectively. With the criterion $\left|\ (\Delta p_i-\Delta p_{i-1})/\Delta p_{i-1}\ \right|$ <1%, grid 4 was chosen for the present simulation.

Table 1
Grid independence analysis with γ-$Re_{\theta t}$ transition model at Re=2000

Case	N	N_i/N_{i-1}	Δp (Pa)	$\left\|\ (\Delta p_i-\Delta p_{i-1})/\Delta p_{i-1}\ \right\|$ (%)
Grid 1	168480	--	31994.8	--
Grid 2	306965	1.82	31164	2.60
Grid 3	605085	1.97	30117.8	3.36
Grid 4	1041005	1.72	29242.7	2.91
Grid 5	1861745	1.79	29330.9	0.30
Grid 6	3026685	1.63	29242.9	0.30

Based on the article by Menter et al. [2006], the yplus value for the γ-$Re_{\theta t}$ transition model was less than 1 and the wall normal grid expansion ratio was set to 1.1 in this paper.

Numerical Method The CFD software ANSYS CFX 15.0 was used to numerically simulate the flow through the microchannel. In the simulation, ideal air at 299.15K was selected as the working fluid. Boundary conditions for the six boundaries were specified for this simplified computational domain. At the entrance, the inlet mass flow rate and the air temperature were employed. The outlet boundary condition was set as pressure outlet. Symmetry was assigned for the two symmetrical planes. No-slip boundary condition was imposed on the other two boundaries which were also assumed to be adiabatic and smooth.

RESULTS AND DISCUSSION

Pressure Drop and Friction Factor The pressure drops measured in the experiments and predicted by the simulation are illustrated in Figure 2.

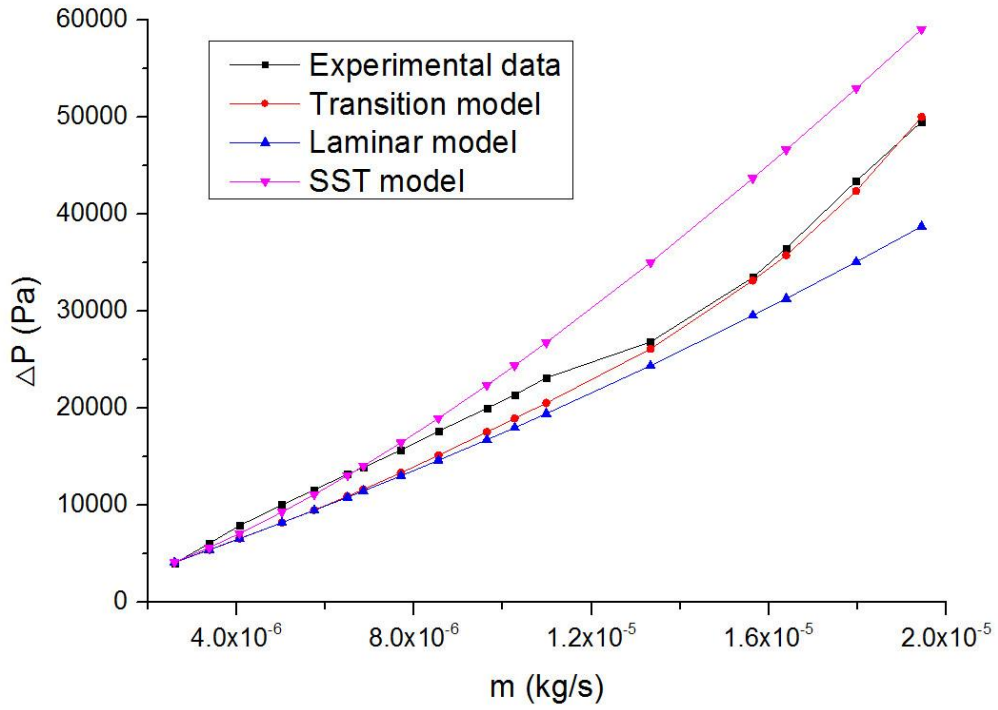

Figure 2. Pressure drop of different models with mass flow rate

As shown in Figure 2, the pressure drops predicted by the SST model are always higher than the pressure drop predicted by the other models. The laminar model and the γ-$Re_{\theta t}$ transition model predict similar pressure drops when the mass flow rate is smaller. The values predicted by the laminar model and the SST model depart further from the experimental data with the increase of the mass flow rate.

The friction factor f is used to compare the data obtained by the different models to the

experimental data. In the experiment. f is calculated by:

$$f = \frac{2\Delta p}{L} \cdot \frac{D}{\rho u^2} \tag{1}$$

where L and D are the length and hydraulic diameter of the channel, Δp is the pressure drop along the channel, ρ and u are the density and velocity of fluid at channel inlet.

The variations of the friction factor predicted by the various models as a function of Reynolds are plotted on a logarithmic scale in Figure 3.

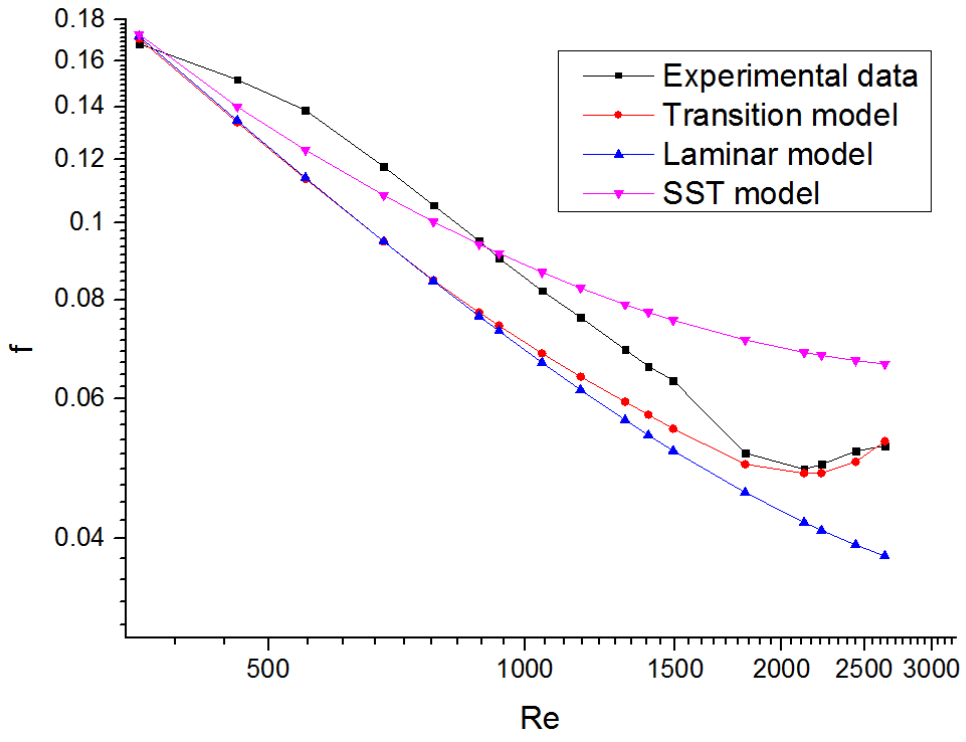

Figure 3. Friction factor of different models with Reynolds number

According to the experimental results, the critical Reynolds number of the flow transition was around 2100. As shown in Figure 3, neither the laminar model nor the SST model predicts the correct trend of transition. The γ-$Re_{\theta t}$ transition model captures the range where the critical Reynolds number lies, nonetheless the predicted values deviates from the experimental ones.

The main reason for the errors in pressure drop and friction factor is considered to be that the numerical simulation computed the pressure drop along the microchannel while in the actual experiments there were pressure losses at the inlet and the outlet. That would make the calculated pressure drops underpredict the true values.

Turbulent Intermittency Figure 4 depicts the distribution contours of turbulent intermittency on the symmetry plane at different Reynolds numbers. In the figure, left of the microchannel is the

inlet and right is the outlet.

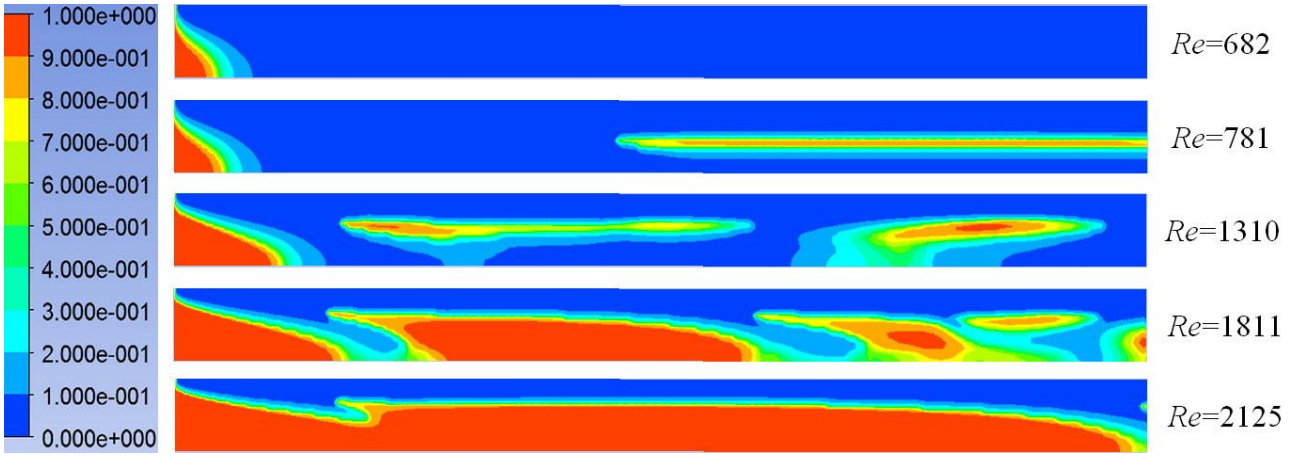

Figure 4. Contours of turbulent intermittency

As shown in Figure 4, for a small Reynolds number, the turbulent region only exists at the entrance of the microchannel due to the inlet turbulence. It is interesting to observe that local turbulent regions appear at the rear of the microchannel before the Reynolds number reaches the critical value. With the Reynolds number increasing, the influence of the incoming flow grows greater. Meanwhile, local turbulent regions appear at the rear of the microchannel. And with the Reynolds number increasing, the streamwise position where the local turbulent regions begin to appear gets closer to the inlet and the regions expand as well. When the Reynolds number is more than 2125, the inlet turbulent region connects with the downstream regions in the microchannel.

According to Figure 4, there are no turbulent regions at the rear of the channel when the Reynolds number is less than 682. This is the reason for the similar simulation results for pressure drop by the laminar model and the γ-$Re_{\theta t}$ transition model at small Reynolds numbers.

Effect of Length-to-diameter Ratio on Transition With the γ-$Re_{\theta t}$ transition model chosen, the effect of length-to-diameter ratio on the critical Reynolds number was studied in this section. In the simulation, the cross-sectional size (0.4mm×0.4mm) of the microchannels was unchanged, as a result, the hydraulic diameter D remained constant. The length of microchannels was changed so the length-to-diameter ratio (L/D) varied.

The flow behavior with L = 10, 30, 40, 50, 70, 90, 110, 200 mm under different Reynolds numbers were simulated and the results are shown in Figure 5. From Figure 5, it can be observed that for $L/D \geq 100$, the transition from laminar to turbulent regime occurs for a Reynolds number in the range 2000-2500, which is consistent with the traditional theory. In the case of L/D=25 or 75 (corresponding to length 10 mm and 30mm), the flow behavior is so strongly influenced by the entrance region that the friction factor shows no abrupt change. The critical L/D value seems to lie between 75 and 100, so $L/D \geq 100$ is suggested to eliminate the influence of the entrance effect in the investigation of microchannel flow.

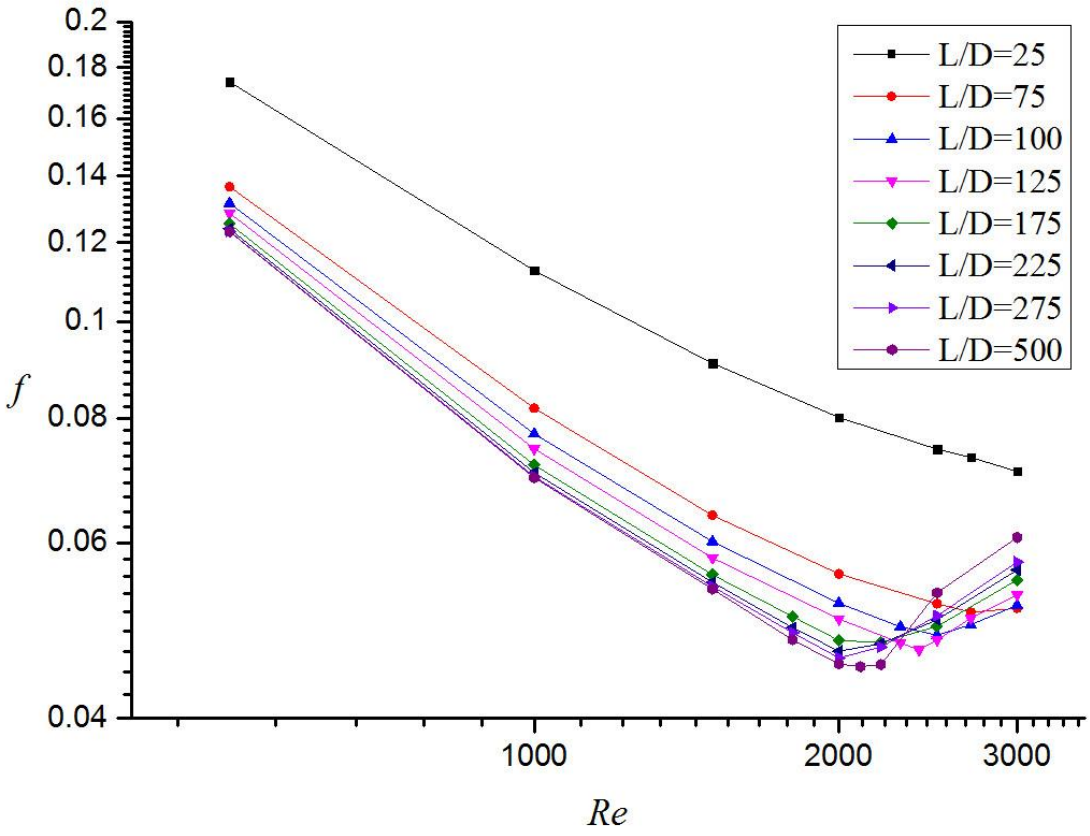

Figure 5. Effect of length-to diameter ratio on the critical Reynolds number

Figure 6 presents the distribution of turbulent intermittency for different length-to-diameter ratios at *Re*=500 and 1000. For *Re*=500, no local turbulent region is observed. For *Re*=1000, the local turbulent regions appear at almost the same streamwise position for different length-to-diameter ratios.

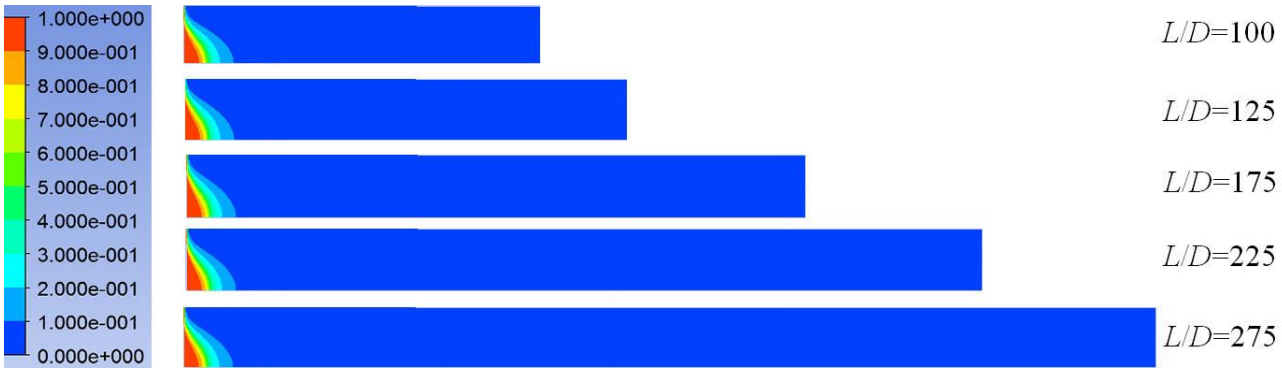

① *Re*=500

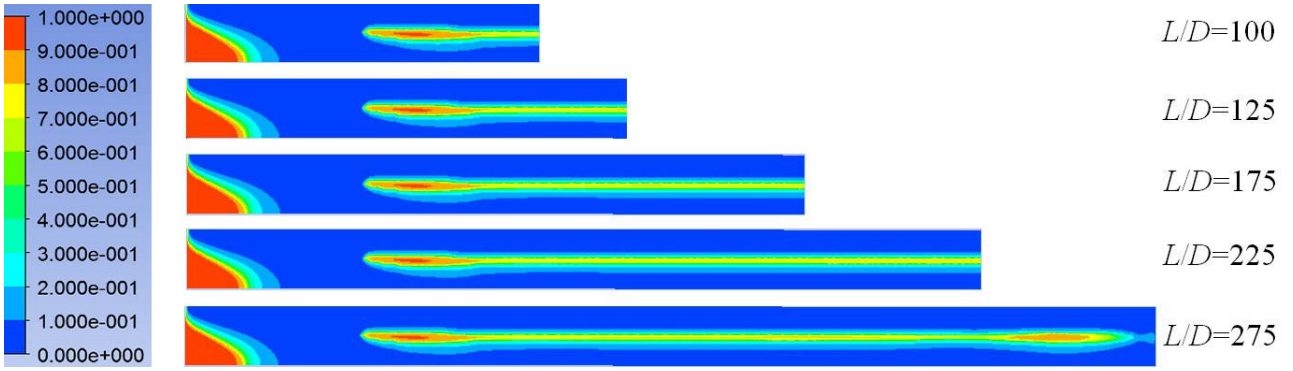

② *Re*=1000

Figure 6. Contours of turbulent intermittency for different length-to-diameter ratios

CONCLUSIONS

Numerical simulation of gas flow in a rectangular microchannel was conducted with the γ-$Re_{\theta t}$ transition model, the laminar model and the SST model. The conclusions are as follows:

(1) In terms of pressure drop, the laminar model and the γ-$Re_{\theta t}$ transition model predict similar results when the mass flow rate is small. When the mass flow rate gets higher, values predicted with the γ-$Re_{\theta t}$ transition model matches best with the experimental data.

(2) Among the three flow models, only the γ-$Re_{\theta t}$ transition model captures the range where the critical Reynolds number lies despite deviations from the experimental data.

(3) According to the contours of turbulence intermittency, before the Reynolds number reaches the critical value, local turbulent regions appear at the rear of the microchannel and the regions expand with increasing Reynolds number.

(4) The transition from laminar to turbulent regime occurs for Reynolds number in the range 2000-2500 for microchannels with $L/D \geq 100$. In the investigation of flow in microchannels, $L/D \geq 100$ is suggested to eliminate the influence of the entrance effect.

REFERENCES

Hu, Y.D., Werner, C. and Li, D.Q. [2003], Influence of Three-dimensional Roughness on Pressure-driven Flow through Microchannels, Journal of Fluids Engineering, Vol.125, No.5, pp 871-879.

Kandlikar, S., Garimella, S., Li, D.Q., et al. [2014], Heat Transfer and Fluid Flow in Minichannels and Microchannels (second edition), Butterworth/Heinemann Publ. Co., Waltham, Massachusetts.

Mala, G.M. and Li, D.Q. [1999], Flow Characteristics of Water in Microtubes. International Journal of Heat and Fluid Flow, Vol.20, No.3, pp 142-148.

Menter, F.R., Langtry, R.B., Likki, S.R., et al. [2006], A Correlation-based Transition Model Using Local Variables—Part 1: Model Formulation, Journal of Turbomachinery, Vol.128, No.3, pp 57-67.

Mokrani, O., Bourouga, B., Castelain, C., et al. [2009], Fluid Flow and Convective Heat Transfer in

Flat Microchannels, International Journal of Heat and Mass Transfer, Vol.52, No.5-6, pp 1337-1352.

Qu, W.L., Mala G.M. and Li D.Q. [2000], Pressure-driven Water Flows in Trapezoidal Silicon Microchannels, International Journal of Heat and Mass Transfer, Vol.43, No.3, pp 353-364.

Rawool, A.S., Mitra, S.K. and Kandlikar, S.G. [2006], Numerical Simulation of Flow Through Microchannels with Designed Roughness, Microfluidics and nanofluidics, Vol.2, No.3, pp 215-221.

Sahar, A.M., Özdemir, M.R., Fayyadh, E.M., et al. [2015], Single Phase Flow Pressure Drop and Heat Transfer in Rectangular Metallic Microchannels. Applied Thermal Engineering, 93, pp 1-13.

Tsien, H.S. [1946], Super Aerodynamics-mechanics of Rarefied Gases, Journal of the Aeronautical Sciences, Vol.13, No.12, pp 653-664.

Toh, K.C., Chen, X.Y. and Chai, J.C. [2002], Numerical Computation of Fluid Flow and Heat Transfer in Microchannels, International Journal of Heat and Mass Transfer, Vol.45, No.26, pp 5133-5141.

Tuckerman, D.B. [1984], Heat-transfer Microstructures for Integrated Circuits, Lawrence Livermore National Lab, CA.

Zhang, J., Diao, Y.H., Zhao, Y.H., et al. [2014], An Experimental Study of the Characteristics of Fluid Flow and Heat Transfer in the Multiport Microchannel Flat Tube, Applied Thermal Engineering, Vol.65, No.1–2, pp 209-218.

Zhu, Z.B., Tao, Z., Tian, Y.T., et al. [2016], Experimental Investigation of the Air Flow Behavior and Heat Transfer Characteristics in Microchannels with Different Channel Lengths, *ASME 2016 5th Micro/Nanoscale Heat and Mass Transfer International Conference, 3-6 January 2016 Biopolis*, MNHMT2016-6612.